International Conference on Space Optics—ICSO 2022

Dubrovnik, Croatia

3–7 October 2022

Edited by Kyriaki Minoglou, Nikos Karafolas, and Bruno Cugny,

10 Gbauds digital optical link and analog link from/to geostationary satellite

10 Gbauds digital optical link and analog link from/to geostationary satellite

Sylvain Poulenard[a1], Thomas Anfray[a], Michael Crosnier[a], Jean-Frédéric Chouteau[a], Jordane Thouras[a], Charles-Ugo Piat[a], Jean-Adrien Vernhes[a], Laurent Coret[a], Walid Atitallah[a], Alassane Dupuy[a], Louis Barbier[a], Lyonel Barthe[a], Benjamin Gadat[a], Thomas Dreischer[a], Etienne Samain[b], Erick Bondoux[b], Thierry Lanz[b], Frédéric Lacoste[c], Julien Sommer[c], Géraldine Artaud[c], Alain Dominique Thomas[d]

[a]Airbus; [b]OGS Technologies; [c]Centre National d'Etude Spatial ; [d] Safran Data Systems

ABSTRACT

Architecture of a 10 Gbauds link between new high complexity optical ground station suitable for feeder link and a geostationary satellite is described. Such link is tested in laboratory environment with emulation of power fluctuations representative of the power budget between the optical ground station and the satellite. The software and hardware developed reach the expected performance and the system performance model is demonstrated to be accurate at 1 dB.

Keywords: Optical communications, optical satellite feeder link, OOK, DPSK

1 INTRODUCTION

Optical communication links at 1.55 µm are foreseen to be a valuable alternative to the conventional radio-frequencies links between the spacecraft LEO/GEO and a fixed Earth ground station for missions such as Internet delivery, Earth observation data download, and Deep Space data download. Such links present the technical challenge of crossing the atmosphere where clouds and turbulences impair the transmission. Regarding LEO Earth observation downlink and Deep Space data download, the Consultative Comity for Space Data System (CCSDS) sets up working groups for standardization of such optical links [1], and demonstrations have been running in many countries [2]-[5].

Regarding the mission of broadband access for Internet delivery, European space agencies and European Commission have financed system studies to evaluate technological feasibility of GEO optical feeder links [6][7] as well as hardware development [13]. In 2016, the European Space Agency has launched the HydRON (High Throughput Optical Network) project targeting optical interconnections in the Tb/s regime for inter-satellite links and feeder links [8]. For GEO feeder links, the optical band presents the advantages of tremendous bandwidth capacity and no interference but also the drawbacks of being blocked by clouds and strongly distorted by the atmospheric turbulence when it crosses the atmosphere. Cloud blockages are commonly mitigated by site diversity between Optical Ground Stations (OGS) geographically spread over the coverage area [7]. Atmospheric turbulence impacts are mitigated thanks to the implementation of adaptive optic system at each OGS reducing signal power fading [9][10] and thanks to the usage of a protection scheme to retrieve the information corrupted by errors during the transmission.

In 2019, Airbus Defence and Space and its partners presented breadboard of communication chain equipment [13] and presented protection schemes for the GEO feeder links [11].

Airbus Defence and Space and CNES are now planning a demonstration between new optical ground stations larger or equal to 50 cm with adaptive optic systems and the new Airbus medium size optical terminal (TOP-M) embarked on a GEO satellite (the TELEO in-orbit demonstrator). The TOP-M includes the flight models of communication chain equipment. The main objectives of such demonstration are the evaluation of the flight hardware performance, the optical links budgets calibration (uplink and downlink) including the impact of atmospheric turbulences with adaptive optics, the 10 Gbauds optical communication chain performance demonstration. The hardware development is currently on-going under a very challenging planning.

---

[1] sylvain.poulenard@airbus.com; Tel: + 33562196472; Airbus Defence and Space, 31 rue des Cosmonautes Toulouse.

The paper is organized as follows: §2 presents the links architecture between optical ground station and the on-board terminal TOP-M, §3 presents the on-board terminal TOP-M, §4 presents the on-ground optical terminal, §5 presents the communication hardware under test, §6 presents the test setup for the digital uplink and digital downlink, §7 presents the communication chain performance (Bit Error Rate before decoding and Frame Error Rate (FER) after decoder), §8 presents the link margin model accuracy, §9 is the conclusion.

2 LINKS ARCHITECTURE

2.1 Digital downlink

A digital downlink is in charge of downloading great volume of space optical telemetry to avoid the RF telemetry bottleneck. A pseudo random binary sequence (PRBS) mode is also implemented to derive bit error rate (BER) performance (before and after on ground decoder). The downlink optical modulator is implemented in the Terminal Control Electronic (TCE). The generated 10 Gbauds baseband signal is provide at the transmitting Laser Communication Electronic (LCE-TX) input presented in [15] by iXblue. The LCE generates low power non-return to zero differential phase shift keying (NRZ-DPSK) signal around 1560 nm. This low power signal is amplified by the booster amplifier up to 5 W continuous power, described in [16] by CILAS. The On-Board Terminal sends the signal down to the On Ground Terminal. The On Ground Terminal collects the signal and injects it into a single mode fiber interfacing with the receiving Laser Communication Electronic (LCE-RX). The LCE-RX detects the optical signal and provide it to the Optical Modem RX.
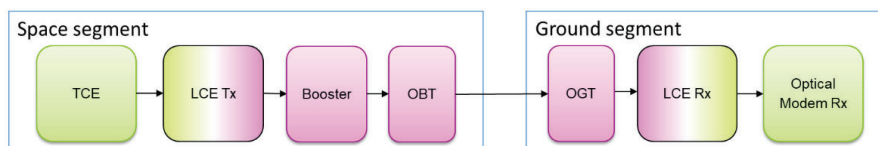

Figure 1. Digital downlink architecture

2.2 Digital uplink

A digital uplink allows deriving BER performance and might allow file uploading in the future. The uplink optical modulator is implemented in the Optical Modem TX made by Airbus Defence and Space. The generated 10 Gbauds baseband signal is provide at the on-ground LCE-TX input designed by iXblue. The LCE-TX generates low power non-return to zero on-off keying (NRZ-OOK) signal around 1550 nm. This low power signal is amplified by a ground booster amplifier up to 10 W and maybe 30 W continuous power. The On Ground Terminal sends the signal up to the On Board Terminal. The On Board Terminal collects the signal and injects it into a single mode fiber interfacing with the LCE-RX presented in [15] by iXblue. The LCE-RX detects the optical signal and provides it to the uplink demodulator designed and implemented by Airbus Defence and Space in the TCE.
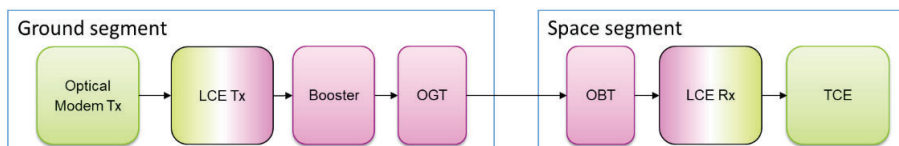

Figure 2. Digital uplink architecture

2.3 Analog uplink

An analog uplink is also implemented for a transparent optical feeder link proof of concept for broadcast system and to allow uplink carrier to noise ratio estimation on-board the satellite at the LCE-RX output with around 0.5 dB accuracy. The Software Defined Radio (SDR) TX modem generates a 40 MHz large DVB-S2 signal in L-band which is then transposed around 1550 nm by amplitude modulation (reduced carrier single side band or dual side band) thanks to the Analog Modbox TX. The resulting signal goes through the booster, the on-ground terminal, the on-board terminal and the LCE-RX like the digital uplink signal. At the terminal control electronic, the 40 MHz DVB-S2 signal is digitalized, encapsulated and sent back to the on-ground SDR DVB-S2 modem RX. The overall link from/to SDR DVB-S2 MODEM is protected by an upper layer forward error code (FEC) designed by Airbus Defence and Space. The concept of upper layer FEC to

protect video transmission has already been studied [16]. Nevertheless, it would be the first end to end demonstration up to our knowledge.
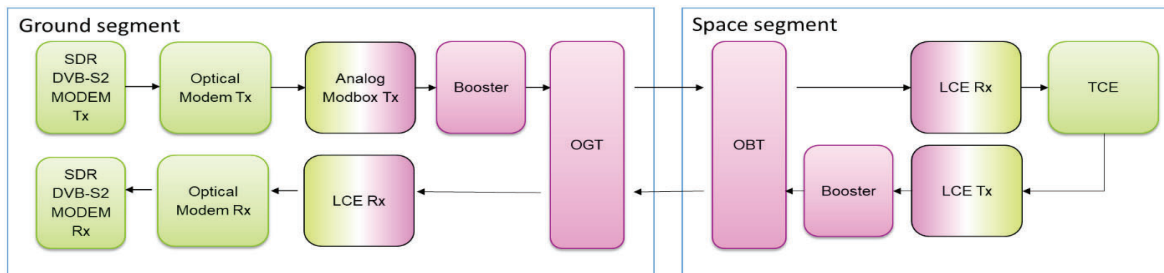

Figure 3. Analog uplink architecture

3 ON-BOARD TERMINAL

3.1 Global description

The optical on-board terminal (OBT) is composed of several parts:

- Terminal Control Electronic (TCE). TCE manages the entire optical communication terminal (startup, stop, monitoring, failure, etc.). It includes electronic board, also called Optical Modem, dedicated to the 10 Gbaud electrical signals digital processing and generation. The Optical Modem is also capable to analyze the data after the transmission in order to compute the BER for link quality assessment (monitoring purpose).
- Laser Communication Electornic (LCE). It is composed of the electro-optic transmitter (TX) and the opto-electronic receiver (RX). It allows the electrical data conversion into optical data and vice-versa. It also analyzes the power injected into the opto-electronic receiver (RX) input fiber.
- Laser Power Electronic a.k.a. Booster. The booster is an optical amplifier used just after the LCE-TX in order to increase the optical power for enabling the transmission over long distances.
- Focal plane assembly (FPA). This is the interface between fibered optics and free space optics. It includes the TX/RX duplexing, the fiber injection mechanism and a part of the acquisition and tracking system.
- Terminal Proximity Electronic (TPE). It manages all the FPA electronic, more information presented in [18].
- Telescope (TEL). The telescope is the interface between the terminal and the free space channel. It includes all the necessary optics and the other part of the acquisition and tracking system. More information can be found in [18].

3.2 Uplink received irradiance

The uplink irradiance power can be monitored by the TOP-M acquisition and tracking sensor at a frequency superior to 1 kHz. The accuracy is expected to be better than 1 dB over a range greater than 20 dB.

3.3 Uplink injected power monitoring

The uplink injected power can be monitored by the on-board LCE-RX at a frequency of 20 kHz. Such feature has been tested under relevant power time series injected into the LCE-RX fiber for a GEO feeder link pre-compensated uplink. Figure 4 depicts the power error distribution of the estimator. It shows that more than 93% of the time series can be retrieved with error less than 0.5 dB.
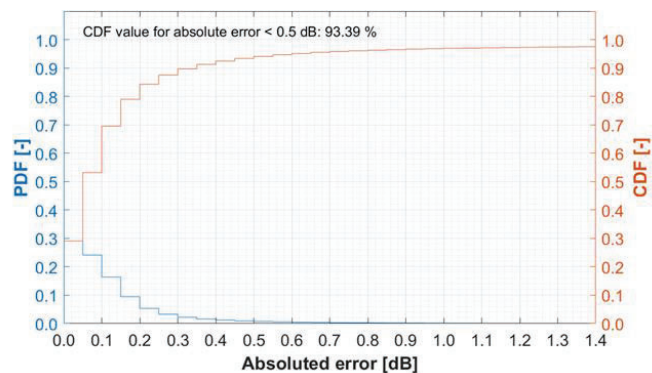

Figure 4. Absolute error on power injected into the LCE-RX for a worst case uplink power fluctuation

4 OPTICAL GROUND STATIONS

4.1 French OGS (FrOGS)

In the frame of DYSCO project, the FrOGS consortium (CNES, and the companies, Safran Data System, OGS Technologies, ALPAO, and Airbus Defence and Space) is currently developing an optical ground station (OGS) for demonstrating optical communications in free space and, more particularly adapted to the cases of GEO feeder links and TMI-LEO downlinks. This development is supported by CNES and co-financed by the aforementioned manufacturers. FrOGS will be located at Observatoire de la Côte d'Azur, Calerne.
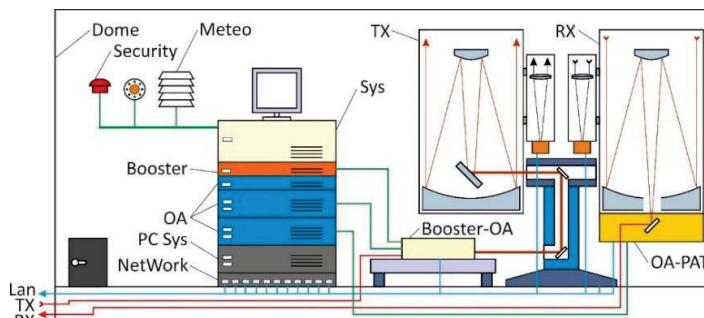

Figure 5: Schematic architecture of the FrOGS station, developed by the French consortium (CNES, ADS, ALPAO, OGS Technologieset SDS)

The OGS is based on a bi-static architecture with an Alt-Az mount supporting both the TX laser emission optics and the RX satellite stream reception optics (Figure 5 and Figure 6). The transmitting and receiving optics are compact 500 mm diameter telescopes designed with a rigid, light and stable mechanical structure.

The focal instrumentation of each optical tube consists of a Pointing-Acquisition-Tracking (PAT) system, a fine-pointing device (tip-tilt mirror) and high-resolution adaptive optics (AO) system. The AO system is based on a deformable mirror and a Shack-Hartmann wave front analyzer. Each adaptive optics is independently slaved to the RX optical stream received by the two telescopes. The TX optical setting also includes a forward pointing system based on a second tip-tilt mirror allowing for the satellite velocity aberration compensation.

The RX focal instrumentation is directly coupled at the RX telescope Cassegrain focus and embarked behind the primary mirror. The opto-mechanical interface at the focal RX instrumentation output is designed to allow coupling with a single-mode optical amplifier for GEO feeder links or with a detector in free space for the TMI-LEO links.

The TX instrumentation is located on the lower floor in an environmentally-controlled focal laboratory. It connects the TX upstream generated by a 43 dBm power fibered amplifier (booster) with the TX telescope through a motorized coudé optical train.

In parallel to the TX and RX optics, the OGT incorporates two 100 mm bezels, respectively for beacon functions (continuous laser diode amplified by a 40 dBm fiber amplifier) and wide-field sensor (visible and infrared imaging sensor).

The telescope mount is driven by DirectDrive motors combining speed for LEO tracking and pointing stability at the µrad level. The entire OGS is protected by a slit dome on the roof

Figure 6. CAO view of the instrument optics on the Alt-Az mount

of a 4 x 4 m size building. The station can be operated locally or remotely through a secure link.

The baseline architecture of the demonstration carried out in the frame of the DYSCO project relies on this French OGS in order to assess its ability to efficiently mitigate atmospheric effects on a long-term basis. This demonstration prototype should be a precursor of further operational OGS.
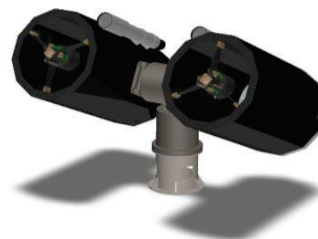
4.2 Airbus OGS (A-OGS)

Airbus Netherlands is providing an OGS solution for GEO feeder link demonstration via the ScyLight activity CREOLA. This solution is split into three phases, in a step-by-step approach. In Phase 1, Airbus will operate the already validated ESA OGS with support of its partner GA-Synopta. In Phase 2, Airbus will add its own adaptive optics corrected TX-OGS in a transportable configuration, together with partners ASA and TNO. Combined with ESA OGS, a bi-directional feeder link is then operated. In phase 3, Airbus will demonstrate a bi-directional feeder link with a monostatic OGS, based on an RX/TX AO system from partner GA-Synopta.

4.2.1 Short term bi-static approach

The chosen bi-static architecture allows for a gradual growth in link complexity. OGS key technologies will be demonstrated in genuine space-ground link conditions, providing valuable feedback for OGS product designs.

An important objective is to validate the predicted efficiency of full-aperture RX-AO and pre-compensated TX-AO on a 20 cm uplink communications beam in the 1550 nm band. Over a genuine GEO satellite atmospheric channel, tests in different atmospheric conditions will lead to a comprehensive optical channel analysis.

Local atmospheric turbulence at the telescope level is considered as a major cause that disturbs an AO system performance. Those turbulence are induced by surface layer's flow distortions and local thermal turbulence from nearby infrastructure elements. Predictions on associated AO performance degradation for a transportable OGS, with a large aperture telescope in a tight dome enclosure, do not exist yet. Phase 2 collects measurements to characterize local turbulence contributors and their related AO impact, to validate key parameters of future OGS products.

Figure 7. Bi-static OGS approach for Phases 1 & 2

4.2.2 Monostatic OGS prototype

The monostatic OGS (M-OGS), carried out in the third phase, constitutes a platform that provides all functions for bi-directional GEO optical feeder link testing.

To minimize transport overhead, the M-OGS will be tested in a stationary OGS environment at Zimmerwald site location in Switzerland. At a lower site altitude, but at almost identical zenith angle to TELEO, this allows for a comparison of fundamental findings from Phases 1 and -2, collected at Izana site on Tenerife.

The M-OGS provides full aperture RX-AO over 80 cm, combined with AO/based TX-pre-compensation for two TX beams of 20 cm diameter. The AO module form factor allows a later integration in a transportable container, like demonstrated in Phase 2.

The M-OGS will re-use the external beacon module from Airbus NL, and it will implement parts of the OGS Control and Safety System, already tested during in-orbit demonstration phase 1.
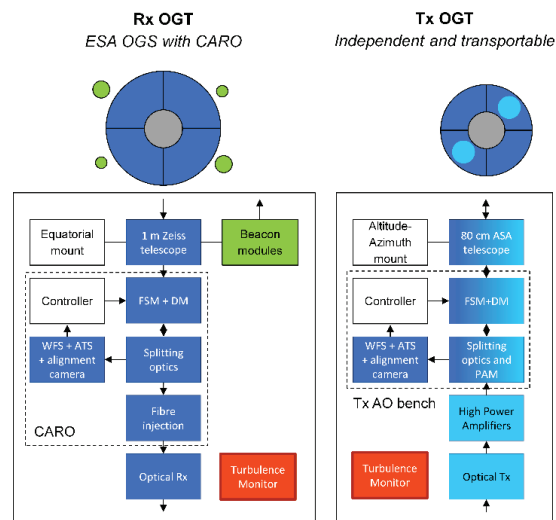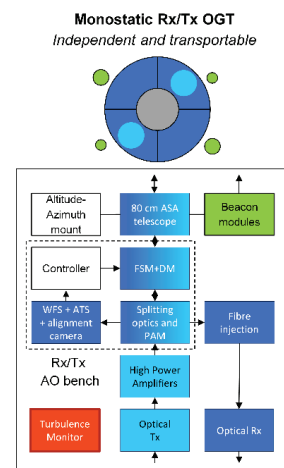

Figure 8. Monostatic OGS for Phase 3

5 HARDWARE UNDER TEST

5.1 Space segment

5.1.1 Terminal Control Electronic

An equivalent model of the terminal control electronic presented in [18] is used for generating or analyzing pseudo-random data. It only includes the processing board which implements the FEC, interleaver and framing.

5.1.2 Laser Communication Electronic

Figure 9 presents a picture of the LCE demonstration model.

The LCE allows the conversion of the electrical data into optical data and vice-versa. It interfaces electrically with the DPU part of the TCE and optically with the focal plane assembly and the booster. It is managed directly by the TCE.

The LCE is composed of three electronic boards:

Figure 9. Picture of space grade LCE

- **DC/DC converter board.** It aims at converting the primary unregulated 100 V bus line distributed by the GEO satellite into specific secondary voltages required by the transceiver. It is composed of a front-end generic converter and a back-end specific converter for modularity.

- **TX board.** Its role is to convert 10 Gb/s NRZ digital electrical data into 10 Gb/s NRZ-DPSK optical signal. The board embarks two optical channel emitters (OCE), one nominal and one in cold redundancy. The OCE is a fully packaged sub-assembly composed of:
  - A continuous wave (CW) distributed feedback (DFB) laser, thermally regulated by a thermo-electrical cooler (TEC) and generating the optical carrier locked at a specific wavelength. The package also includes a monitoring photodiode (PD)
  - A Mach-Zehnder modulator (MZM), modulating the optical carrier
  - A RF driver, composed of three amplification stages for DPSK modulation, able to amplify the signal coming from DPU up to the required voltage for the MZM

  Both OCE optical outputs are multiplexed into a single fiber using an optical coupler. After that, an optical coupler and a shared monitoring photodiode (over the two channels) allows picking up small amount of optical power to perform the modulator bias loop control.

- **RX board.** It amplifies the weak optical signal captured by the telescope and injected into the receiver fiber and perform the opto to electrical conversion. It is composed of a low noise optical amplifier (LNOA), an all-fibered demultiplexer and three optical channel receivers (OCR). OCR are photoreceivers able to demodulated both OOK digital optical signals and intensity modulated analog optical signals depending on their operating gain parameter. One OCR is dedicated to demodulate 10 Gb/s NRZ-OOK optical signal and the two other OCR, one nominal and one in cold redundancy, are devoted to demodulate analog optical signals with a bandwidth from few hundreds of kHz up to 23 GHz.

  LNOA includes also an input monitoring photodiode able to estimate the optical power injected from the focal plane assembly into the optical communication chain receiving fiber with a 10 kHz bandwidth and a dynamic range around 25 dB. This will allow estimating the uplink turbulence effect on the optical power injected into the optical communication chain.

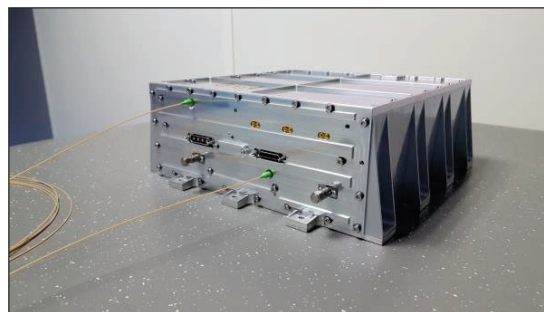Basically the specification of the LCE unit are presented in Table 1.

Table 1. On-board LCE main features

Feature	Specification
Power bus input	• 100 V bus
Controllability	• CAN, analog telemetries
RF input	• 10 Gb/s NRZ electrical signal Single ended 150 mVpp min eye amplitude
TX optical output	• Single mode polarization maintaining fiber • 10 Gb/s NRZ-DPSK optical signal
RX optical input	• Single mode fiber • 10 Gb/s NRZ-OOK optical signal • 500 kHz to 23 GHz analog bandwidth
RF output	• 10 Gb/s NRZ electrical signal Differential 1000 mVpp max eye amplitude • Analog electrical signal Single ended
Wavelength plan	• OCE1: 1562.64 nm nominal channel • OCE2: 1561.01 nm backup channel • OCR1: 1550.12 nm backup analog channel • OCR2: 1548.51 nm nominal analog channel • OCR3: 1546.92 nm nominal digital channel
RX input optical power monitoring	• Range: 25 dB • Bandwidth: 10 kHz
Electrical power consumption	• For all OCE and all OCR: 27.9 W • For 1x OCE and 1x OCR: 21.3 W

More information can be found in [15].

5.1.3 Laser Power Electronic

Figure 11 presents a picture of the LPE demonstration model.

The booster is composed of a main electronic board embarking the DC/DC converter and the control processor, an opto-electronic mezzanine and a baseplate onto high dissipative elements are reported.

Optical amplification up to 5 W continuous power with wall-plug efficiency of around 11% (beginning of life) is based on two amplification stages:

- Stage 1: pre-amplifier. Low power single mode pump diodes are used for this stage. This amplification stage aims at shaping the optical spectrum for the second amplification stage and increasing the signal power for power-amplification.

Figure 10. Picture of the space grade LPE

- Stage 2: power-amplifier. High power multi-mode pump diodes are used for this stage. This amplification stage aims at increasing the signal power up to the required power with required noise factor and providing good spectrum flatness.

Three monitoring photodiodes (PD) are used to monitor the optical signal and to secure the booster operation (input power, inter-stage power and output power). Thermistors are also used to monitor temperature on different components in order to protect them against overheating.

The booster communicates directly with the TCE through CAN link.

Table 2 presents the main specifications of the on-board booster.

Table 2. On-board LPE main features

Feature	Specification
Power bus input	• 100 V bus
Controllability	• CAN, analog telemetries
Optical input	• Min: 6 dBm
Operation wavelength	• From 1555.7 nm to 1565.5 nm
Output power	• From 0 up to 5 W continuous power • Stability <±0.3%
Wall plug efficiency	• 11.2% at 5 W BOL

More information can be found in [16].

5.2   Ground segment

5.2.1 Laser Communication Electronic

The LCE-TX and LCE-RX described in [13] are used as equivalent model for ground equipment.

5.2.2 Optical Modem RX

Figure 12 presents a picture of the Lasercom digital processing unit. The lasercom Rx multi-mission modem performs digital processing from Rx photodetector output up to payload bits delivery on TCP/IP. In the framework of this paper the lasercom modem processes the RF output of the LCE-Rx and delivers payload bits on 10Gbps Ethernet and on 10TB HDD.

Figure 11: Picture of the Lasercom modem

The lasercom is composed of 4 main parts (see figure 13):

1. **Cortex HDR server**. This part is composed of a 4U chassis equipped with a server board driving DSP boards and providing legacy HDR FTP and TCP/IP interfaces.
2. **Acquisition board**. The role of this board is to digitized the 10Gbps DPSK RF signal converted by the photo-detector (LCE-Rx).
3. **Signal Processing board**. This board performs the following functions:
   a.   Resampling and matched filtering
   b.   Clock recovery
   c.   Despreading
   d.   LLR computation fitting any OFE (EDFA+PIN, APD, …)
   e.   Deinterleaving up to 8GB
   f.   Provide channel metrics synchronized with demodulated data: ROP, SNRe, electrical level.
4. **FEC board**. This board is dedicated to channel decoding and data integrity. In the framework of this paper, it performs QC-LDPC decoding, BCH and CRC checking.
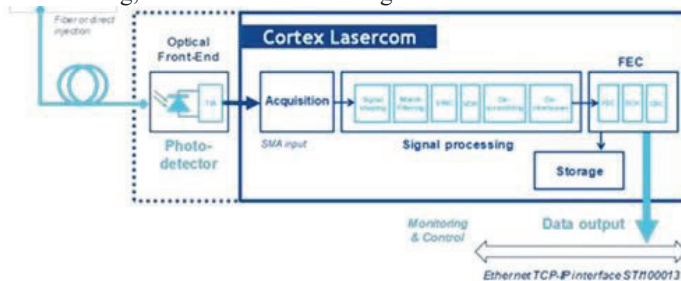

Figure 13 : Cortex Lasercom overview

6 TEST BENCHS

For all the setup, the OBT, the OGT and the channel in between are emulated by a Variable Optical Attenuator (VOA) and a High Speed Variable Attenuator (HS-VOA). These two VOA are controlled so that the Received Optical Power (ROP) function of time at the LCE-RX input corresponds to the operational link scenario. The ROP function of time is computed from a system model and from ONERA's wave optic software [12]. In all this paper, the ROP is defined as the mean optical power per channel measured at the LNOA first amplification stage of the LCE-RX.

6.1 Digital downlink

Figure 12 presents the test bench for the digital downlink scenario. The LCE-TX and booster are electrically powered by 100 V lab source. They are controlled through graphical user interfaces on a computer with CAN and UART probes. TCE-EM realizes the FEC encoding, interleaving and framing. At the receiver side, the LCE-RX is used to demodulate the optical signal which is then transmitted to the optical modem RX. The Optical Modem RX-EM performs synchronization, deframing, desinterleaving, and decoding in order to retrieve the initial useful data.
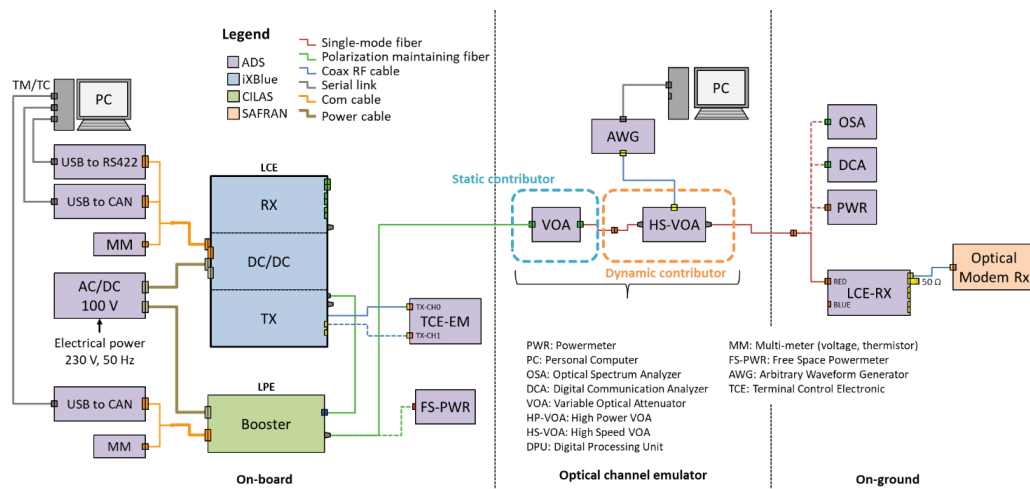

Figure 12: Test bench for digital downlink

6.2 Digital uplink

Figure 13 presents the test bench for the digital uplink scenario. On the on-ground side, the DPU-TX generates either PRBS $2^{63}-1$ or encoded and interleaved data to be transmitted. The 10 Gb/s raw NRZ signal modulates the on-ground optical transmitter breadboard. The LCE-TX output is a 10 Gbaud NRZ-OOK signal at 1546.92 nm. A commercially of the shelf optical booster is used to amplify this signal up to 10 W continuous power. The received signal is demodulated by OCR3 of LCE and converted back into electrical signal processed by the TCE DPU board.
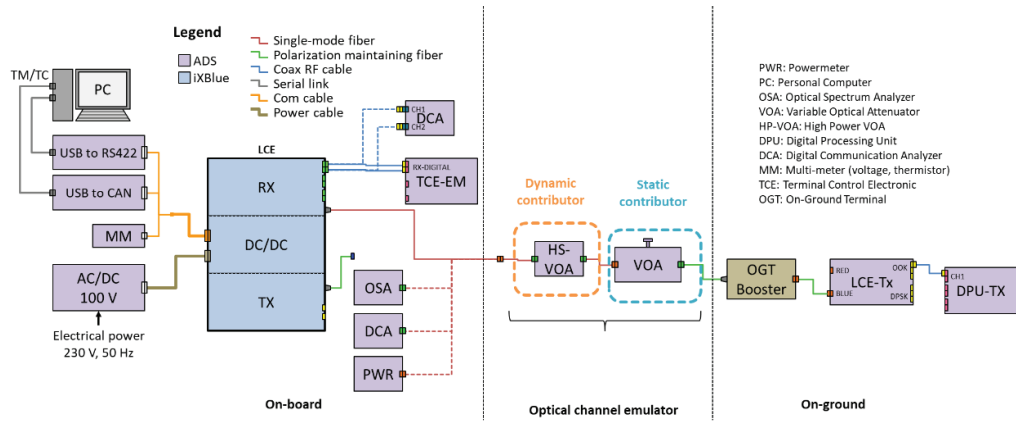
Figure 13: Test bench for digital uplink

7 COMMUNICATION CHAIN PERFORMANCES

7.1 Bit error rate before decoding

Uncoded downlink bit error rate (BER) versus received optical power (ROP) are presented on Figure 14. Uncoded data is based on pseudo-random binary sequence (PRBS) of length 2^{63}-1.

Both downlink channels have the same performance and the overall communication chain presents a state-of-the-art sensitivity of -45 dBm for a BER of 10^{-3}.

Uplink uncoded BER versus ROP for 10 W booster output is shown on Figure 15. An overall communication chain sensitivity of -41 dBm is reached for BER of 10^{-3}.
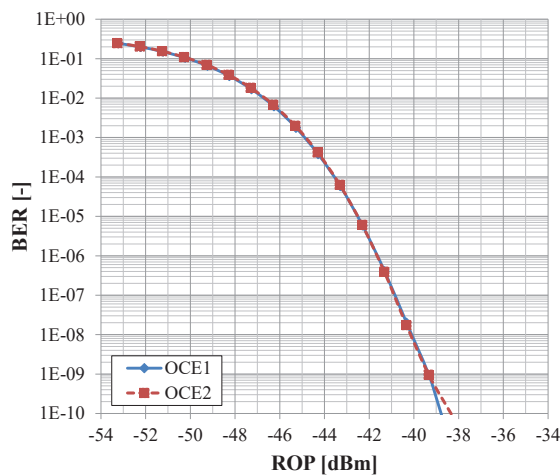

Figure 14: Uncoded downlink BER for 5 W booster output power, 10Gbauds, NRZ-DPSK
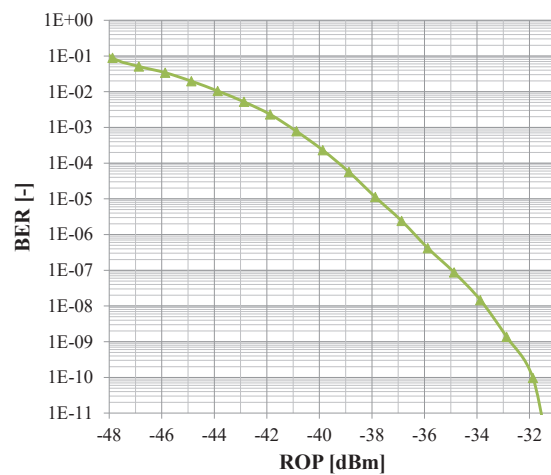

Figure 15: Uplink uncoded BER for 10 W booster output, 10Gbauds, NRZ-OOK

7.2 Frame error rate after decoding

7.2.1 Digital downlink

Figure 16 depicts the FER after decoding for the new LDPC codes presented in [19]. It shows that simulator in floating point and measurement on test bed with the hardware presented in the previous sections § 5 are aligned with 0.3 dB except for the MODCOD with a FEC ratio of 3/10 and a spread factor (SF), also called repeat factor, of 4.
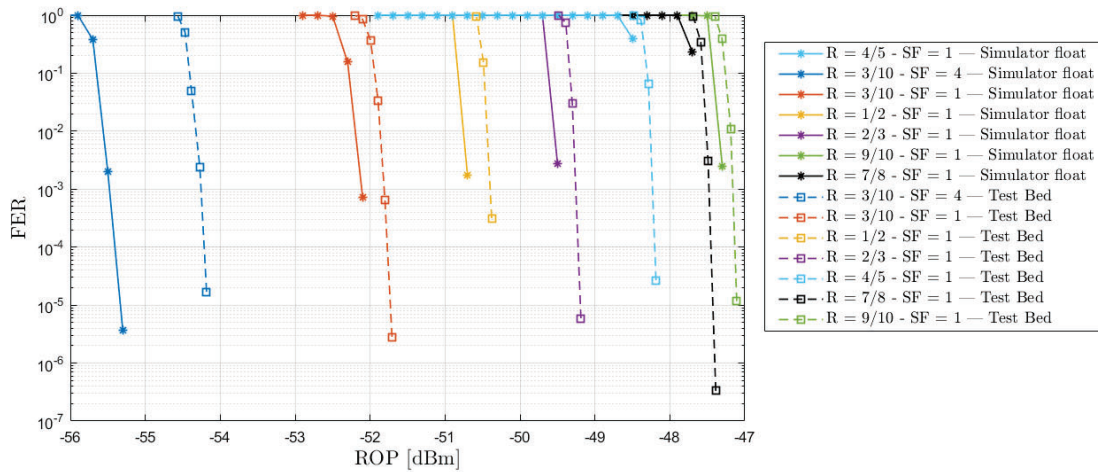

Figure 16. Downlink FER for 5 W booster output power

7.2.2 Digital Uplink

Figure 15 depicts the FER after decoding for the QC-LDPC codes presented in [20]. The useful data rate is limited on the uplink with a repeat factor of 8 due to TCE resources limitations. A quasi-error free FER (FER < 10^{-6}) is obtained for ROP of -50 dBm with QC-LDPC codes R = 1/2 and SF = 8.
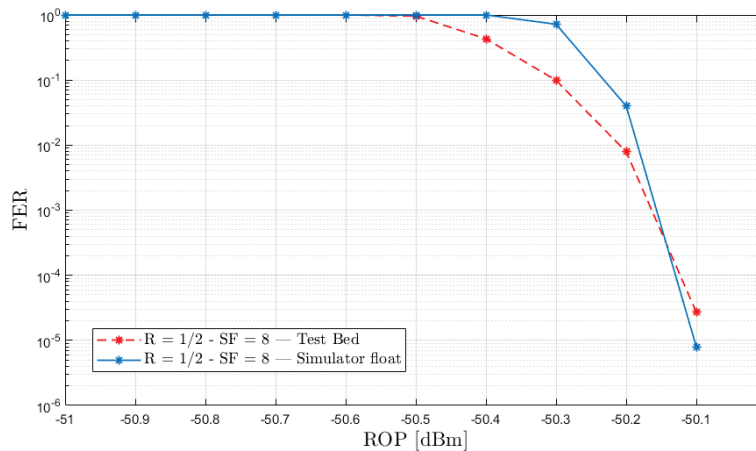

Figure 17. Uplink FER for 10 W booster output power

8 COMMUNICATION LINK MARGIN MODEL ACCURACY

Power margin can be found on test bed by increasing the long term average attenuation over time with the VOA up to finding FER greater than 10^{-5}. In a similar way, the power margin can be computed by the simulator by lowered the time series of received optical power at the input of the LCE-RX. The results of such exercise is provided in the table below for a worst case of turbulence and atmosphere transmission (molecular absorption, diffusion by aerosol and cirrus attenuation) for a configuration of FrOGS presented in § 4.1. It results that simulator can anticipate power link margin with an accuracy of less than 1 dB.

Table 3. Comparison between power margins computed by Simulator versus the ones measured on the test bed.

	Power margin Simulator [dB]	Power margin Test bed [dB]	Delta[dB]
R = 3/10 - SF = 1 - 100ms	7.0	7.6	0.6
R = 2/3 - SF = 1 - 100ms	4.5	5.3	0.8
R = 9/10 - SF = 1 - 100ms	2	2.9	0.9

9 CONCLUSION AND NEXT STEPS

The development phase of the hardware and software of new optical ground stations larger or equal to 50cm with adaptive optic systems and of the new Airbus medium size optical terminal (TOP-M) is currently on going. The communication chain equipment has been tested with equivalent models or even flight models. The performances reaches the expectations and the communication link margin model accuracy stands below 1 dB once the received optical power time series is known. The space segment will allow optical power fluctuation measurement with a range of 20 dB at a frequency greater than 1 kHz.

ACKNOWLEDGEMENTS

REFERENCES

[1] CCSDS Standardisation in Optical Communication, https://artes.esa.int/sites/default/files/08%20-%20Klas-Juergen%20ESA.pdf, 2017.

[2] A. Biswas, B. Oaida, K. S. Andrews, J. M. Kovalik, M. Abrahamson, and M. W. Wright, "Optical payload for lasercomm science (OPALS) link validation during operations from the ISS," in Proc. SPIE, 2015, vol. 9354.

[3] C. Fuchs et al., "OSIRISv1 on Flying Laptop: Measurement Results and Outlook", ICSOS 2019.

[4] H. Taenaka, Y. Koyama, M. Akioka, D. Kolev, N. Iwakiri, H. Kunimori, A. Carrasco-Casado, Y. Munemasa, E. Okamoto, and M. Toyoshima, "In-orbit verification of small optical transponder (SOTA): evaluation of satellite-to-ground laser communication links," in Proc. SPIE, 2016, vol. 9739, pp. 3–12.

[5] Boroson, D. M., Robinson, B. S., Murphy, D. V., Burianek, D. A., Khatri, F., Kovalik, J. M., Sodnik, Z. and Cornwell, D. M., "Overview and results of the Lunar Laser Communication Demonstration," Proc. SPIE 8971, p. 89710S (2014).

[6] B. Roy, S. Poulenard, S. Dimitrov, R. Barrios, D. Giggenbach, A. Le Kernec, M. Sottom, "Optical Feeder links for High Throughput Satellites", Proc. ICSOS 2015.

[7] Sylvain Poulenard et al. "Digital optical feeder links system for broadband geostationary satellite", SPIE LASE, 2017.

[8] H. Hauschildt et al. "HydRON: High thRoughput Optical Network", ICSOS 2019

[9] N. Védrenne et al., "First experimental demonstration of adaptive optics pre-compensation for GEO feeder links in a relevant environment, ICSOS 2019.

[10] N. Védrenne, J-M Conan, C. Petit, V. Michaud, "Adaptive optics for high data rate satellite to ground laser link ", SPIE Photonic West - Free Space Optical Communication, 2016.

[11] Sylvain Poulenard, Benjamin Gadat, Lyonel Barthe, Ronald Garzón-Bohórquez, "Protection schemes for optical communication between optical ground station and a satellite", COAT 2019

[12] N. Védrenne, J. Conan, M. Velluet, M. Sechaud, M. Toyoshima, H. Takenaka, A. Guérin, and F. Lacoste, "Turbulence effects on bi-directional ground-to-satellite laser communication systems," in "Proc. International Conference on Space Optical Systems and Applications," (2012).

[13] T. Anfray et al. "Assessment of the performance of DPSK and OOK modulations at 25 Gb/s for satellite-based optical communications", ICSOS 2019.

[14] Jean-Marc Conan et al. "Adaptive optics for GEO-Feeder links: analysis of point ahead anisoplanatism impact via reciprocity based models", COAT 2019

[15] Clément Guyot, Arnaud Laurent, Jérôme Hauden,Thomas Anfray, Olivier Pouzargue, 'WDM Optical Front End for GEO-Ground for Digital and Analog Telecommunications', ICSOS 2022

[16] Schmitt T., "High power optical amplifier at 1.5 μm for GEO and LEO optical feeder links", ICSO (2022)

[17] Matteo Mazzotti et al, "Analysis of packet level forward error correction for Video Transmission", 2011

[18] Berceau et al. Space Optical Instrument for GEO-Ground Laser Communications, ICSOS 2022

[19] Benjamin Gadat, Lyonel Barthe, Balazs Matus, Charly Pouillat, "LDPC Codes with Low Error Floors and Efficient Encoding, to be published.

[20] Vincent Pignoly, Bertrand Le Gal, Christophe Jego, Benjamin Gadat, "High speed LDPC decoding for optical space link",27th IEEE International Conference on Electronics, Circuits and Systems (ICECS), 2020